Original Research

Reduction and Enrichment of Uranium after Biosorption on Inactivated *Saccharomyces cerevisiae*

Wei Zhang[1, 2], Faqin Dong[3]*, Mingxue Liu[4], Huaiqing Song[5], Xiaoqin Nie[6], Tingting Huo[3],Yulian Zhao[3], Pingping Wang[3], Yilin Qin[3], Lin Zhou[3]

[1]Research Center of Laser Fusion, China Academy of Engineering Physics, Mianyang, China
[2]Analytical and Testing Center, Southwest University of Science and Technology, Mianyang, China
[3]Key Laboratory of Solid Waste Treatment and Resource Recycle, Ministry of Education, Mianyang, China
[4]School of Life Science and Engineering, Southwest University of Science and Technology, Mianyang, China
[5]School of Environment and Resource, Southwest University of Science and Technology, Mianyang, China
[6]School of National Defense Science and Technology, Southwest University of Science and Technology, Mianyang, China

Abstract

Microorganisms not only have a strong biosorption capacity but also can achieve tremendous volume reduction effects for radionuclide wastes. Batch experiments were conducted to investigate the biosorption characteristics of uranium on inactivated *Saccharomyces cerevisiae* and the volume reduction and enrichment of uranium after biosorption were also studied in combination with the ashing method. The results revealed that inactivated *S. cerevisiae* biomass was able to adsorb uranium. The maximum removal efficiency and biosorption capacity for uranium were 96.8% and 31.8 mg/g, respectively. The optimum pH for U(VI) removal was 2.75 and U(VI) biosorption was well described by the Freundlich isotherm model. Thermodynamic investigations showed that biosorption of U(VI) on inactivated *S. cerevisiae* was a spontaneous and endothermic process. In the kinetic studies, U(VI) adsorption on inactivated *S. cerevisiae* reached an equilibrium in 60 min and followed a pseudo-second-order kinetics model. The 100 mg/L of uranium was reduced to less than 0.05 mg/L after 6 rounds gradient descent adsorption, which was enough to meet the National uranium wastewater discharge standards. The ashing experiment demonstrated that ashing process resulted in a large volume and weight reduction ratio as well as enrichment for uranium in the ash. XRD results showed that the species of uranium that existed in the ash were uranium phosphate and $KPUO_6 \cdot 3H_2O$. Waste volume reduction and metal enrichment can be obtained by ashing treatment of the biological absorbent. The method may be beneficial for nuclide and heavy metal disposal treatment in many fields.

Keywords: uranium(VI), inactivated *Saccharomyces cerevisiae*, biosorption, reduction, enrichment

*e-mail: fqdong@swust.edu.cn

Introduction

With the rapid development of nuclear industry, a large amount of radioactive wastewater has been released into the environment [1-3]. Radioactive and toxic U(VI) in wastewater can migrate into the ecosystem, which threatens human health and ecological safety [4-6]. Uranium was classified as a confirmed human carcinogen by the Environmental Protection Agency (EPA) in 1996 [7-8]. Conventional methods of removing uranium pollutants, such as chemical precipitation, ion exchange, solvent extraction, evaporative recovery and membrane separation [9-14] consume large amounts of energy and can cause secondary pollution. They also have low removal efficiency when the ion concentration is less than 100 mg/L [15]. Therefore, it is important to develop efficient, economical and feasible methods for the treatment of uranium contaminated water.

Biosorption, as an alternative method to traditional disposal, has attracted much interest for its high adsorption capacity, low production costs and reduced slurry production [16-17]. In recent years, uranium biosorption by various microorganisms (i.e., bacteria, fungi, yeast, and algae) were reported [18-22] in different laboratories. Current studies have primarily focused on the biosorption characteristics and biosorption mechanisms. *Cladophora hutchinsiae* is low-cost and efficient biosorbent for the removal of U(VI) and the maximum biosorption capacity of *Cladophora hutchinsiae* was found to be 152 mg/g [23]. Living *Saccharomyces cerevisiae* cells were able to adsorb approximately 92% of the uranium in 6-10 h of culturing [24]. Alkali-treated *Lentinus sajor-caju* mycelia increased the bioaccumulation of uranium [25]. The presence of calcium and bicarbonate ions in synthetic groundwater affects the biosorption of uranium by *Arthrobacter* G975 [26]. TEM results showed that bioaccumulation was found to be a potential mechanism involved in uranium biosorption by *Bacillus sp.* dwc-2 and the bioaccumulated uranium was deposited in the cell interior as needle shaped particles at pH 3.0 [27]. The removal of uranium by *Shewanella putrefaciens* was investigated and the results demonstrated the formation of uranium phosphate biominerals, predominantly as chernikovite [$H_2(UO_2)_2(PO_4)_2 \cdot 8H_2O$], on the surface of *S. putrefaciens* cells [4]. As a fungus, *Saccharomyces cerevisiae* is an available by-products in fermentation industry, has strong resistance to metal toxicity and extreme environment conditions compared with other types of microbes. Moreover, *S. cerevisiae* is regarded as an ideal model organism to investigate the interaction between metals and microbes [28]. Therefore, *S. cerevisiae* is a suitable biological adsorbent for metal removal. Microbial activity is an important factor that affects biosorption capacity. There has been much debate over whether to use live or inactivated cells for adsorption. Some researchers advocate the use of active cells for adsorption, as studies have shown that active cells have detoxification functions in the process of biosorption and bioaccumulation [29]. Some laboratory experiments have shown that the ability of inactivated cells to adsorb and enrich toxic metal ions is not worse than that of active cells and can be even higher than that of active cells in some cases. Liu et al. [24] found that inactive cells could absorb more strontium than active cells. However, the selective adsorption of metal ions by inactivated cells is not high when other ions coexist.

Two radioactive waste disposal principles are reduction and immobilization. Reduction (volume reduction or weight reduction) is a precondition for immobilization. In recent years, the development of innovative treatment processes for low and intermediate level radioactive waste has also emphasized volume reduction as one of the main objectives [30]. Volume reduction using an appropriate treatment can decrease the amount of waste to be removed, resulting in a reduction in the disposal cost and enhanced efficiency of the disposal site [31]. Methods that are employed for volume reduction of radioactive waste are incineration, evaporation, crystallization and super-compaction [32-35]. Incineration technology in Korea has been used for the treatment of combustible radioactive waste and the volume reduction ratio achieved was 65 [32]. A combination of membrane and evaporation technologies for the treatment of radioactive wastewater can result in a volume reduction factor higher than 600 [33]. Bykhovskii et al. [34] proposed that selective crystallization could be used to reduce the amount of radioactive waste. Advanced Volume Reduction Facilities (AVRF) in Japan so far have treated 750 m³ by melting or super compaction for low level radioactive solid wastes; the volume reduction ratio was from 1.7 to 3.7 [36]. Removal radionuclides from solution by microorganisms have been described earlier in this paper. However, the reduction effect during the biosorption process has not been well reported.

The aim of the present work is to study the reduction and enrichment of uranium after biosorption using inactivated *S. cerevisiae*. For this purpose, the biosorption characteristics of inactivated *S. cerevisiae* for uranium were investigated. We treated high concentration uranium wastewater using gradient descent biosorption and centrifugation separation under optimal conditions to meet the discharge standards. Finally, the volume or weight of biosorbent was reduced by ashing. The results show that treatment using biosorption and ashing can achieve a large volume or weight reduction and uranium can be enriched in the ash.

Materials and Methods

Preparation of Biomass

Saccharomyces cerevisiae biomass used in present work was purchased from Angel Yeast Co., Ltd., China. The dry biomass was autoclaved at 121ºC for 20 min to

inactivate the cells. The treated biomass was then dried in an oven (40ºC, 2 h) and stored in a desiccator for subsequent use in the batch biosorption experiments.

Preparation of U(VI) Solution

A stock solution of U(VI) (1000 mg/L) was prepared by dissolving 2.1092 g of $UO_2(NO_3)_2 \cdot 6H_2O$ in a small amount of concentrated nitric acid and diluting to 1000 mL. Uranyl hexahydrate ($UO_2(NO_3)_2 \cdot 6H_2O$) was obtained from Beijing Chemical Industry Company, China. Other concentrations of U(VI) solutions were diluted from the U(VI) stock solution. Other chemical reagents used in the experiments were of analytical reagent (AR) grade. All solutions were prepared using deionized water.

Batch Biosorption Experiments

Generally, 0.10 g inactivated *S. cerevisiae* was placed into a series of 100 mL conical flasks containing 20 mL of U(VI) solution with the desired initial U(VI) concentration (5 - 200 mg/L). The number of *S. cerevisiae* cells in the U(VI) solution was approximately 2.8×10^{12} (as determined using a hemocytometer). The initial pH of the U(VI) solution was adjusted with 0.10 mol/L HCl or NaOH. Then these conical flasks were shaken on a water bath shaker at 150r/min at different temperatures (288 – 313 K). Supernatant samples were separated by centrifugation at suitable time intervals and used for testing residual U(VI) concentrations by inductively coupled plasma mass spectrometry (ICPMS, Agilent 7700x). The batch experiment method was performed in triplicate.

U(V) removal efficiency R (%) and biosorption capacity q (mg/g) was calculated according to the following formula:

$$R = \frac{(C_0 - C_t)}{C_0} \times 100\% \tag{1}$$

$$q = \frac{(C_0 - C_t) \times V}{m} \tag{2}$$

...where C_0 (mg/L) is the initial concentration of uranium(VI), C_t (mg/L) the concentration of the uranium(VI) in solution at time t, V (L) the volume of uranium(VI) solution, and m (g) the amount of biomass.

Gradient Descent Biosorption Experiments for Uranium Concentration

On the basis of the best adsorption conditions in the batch biosorption experiments, gradient descent biosorption experiments of a uranium solution were performed. The concentration of uranium in the solution for the first adsorption experiment was 100 mg/L. The initial concentration of uranium solution in each subsequent adsorption experiment was the residual concentration of uranium solution after the previous adsorption experiment. An equivalent amount of inactivated *S. cerevisiae* sorbent was replaced in each gradient descent biosorption experiment and the other experimental conditions were the same as the batch biosorption experiments.

In the study, six rounds gradient descent biosorption experiments were designed. After biosorption, 5 mL of the supernatant was removed to analyze the residual uranium concentration.

Ashing Experiment

To investigate the reduction effect, an ashing experiment of the adsorbent was conducted. After biosorption, the centrifuged samples were washed several times with deionized water to remove the remaining uranium solution and then the centrifuged cells were lyophilized for 24 h. The dried sediment was carbonized in a corundum crucible on an electrothermal furnace before ashing. The carbonization process was performed until no more smoke was released. The corundum crucible was then placed on a brick for cooling to room temperature. The carbonized sample was placed into a muffle furnace at 550-600ºC until the weight of sample did not change. The ashing sample was removed and cooled and was then analyzed by SEM and XRD. Ashing experiments were performed in triplicate.

Volume reduction ratio (V_{RR}) and weight reduction ratio (W_{RR}) were calculated according to Eqs. 3 and 4:

$$V_{RR} = \frac{V_U}{V_{ash}} \tag{3}$$

$$W_{RR} = \frac{W_{sediment}}{W_{ash}} \tag{4}$$

...where V_U (L) is the U(VI) solution volume before biosorption, V_{ash} (mL) is the ash volume, $W_{sediment}$ (g) is the sediment weight, and W_{ash} (g) is the ash weight.

Results and Discussion

Effect of Initial pH on the Biosorption of U(VI)

Solution pH is an important parameter that affects biosorption. The species of uranium ion that exists in solution and the surface charge of microbes are both pH dependent [37]. The effect of pH on the biosorption of U(VI) was performed at pH 1.00-7.00 and the results are shown in Fig. 1. As shown in Fig. 1a), U(VI) biosorption increased in the range of pH 1.00 to 2.75, but decreased over the range of pH 2.75 to 7.00. U(VI) removal efficiency was greater than 90% between pH 2.50 to 3.50, however, this value decreased to 49% at pH 7.00. The maximum U(VI) removal efficiency and biosorption capacity were 95.3% and 16.2 mg/g, respectively, at pH 2.75.

Previous studies have indicated that uranyl ions exist in acid solution mainly in the form of hydrated ions and can form complex ions with HCO_3^-, OH^-, HPO_4^{2-}, PO_4^{3-} and SiO_4^{4-} [38]. The speciation and stability of uranyl ion complexes in solution at pH 1.00-7.00 were simulated using Visual MINTEQ 3.1. As shown in Fig. 1b), at pH≤3.50, the predominant species of U(VI) was positively charged UO_2^{2+} ions. UO_2^{2+} ions were rapidly attracted by electrostatic attraction to the negatively charged surface of the inactivated *S. cerevisiae* cells. However, at very low pH values (pH≤2.00), large quantities of hydrogen ions in solution can compete with UO_2^{2+} for the adsorption sites on inactivated *S. cerevisiae*, leading to lower uranium uptake. At pH 3.50 - 5.00, hydrated species of U(VI) [i.e. $[(UO_2)_2(OH)_2]^{2+}$, $[(UO_2)_3(OH)_5]^+$, $[(UO_2)_4(OH)_7]^+$, $[UO_2OH]^+$ and $[(UO_2)_3(OH)_4]^{2+}$] are dominant in solution. The hydrated species of U(VI) had larger ionic radii and might occupy more adsorption sites when interacting with *S. cerevisiae*, resulting in a decrease in uranium removal. At pH 5.00 - 7.00, $[(UO_2)_3(OH)_5]^+$ and $[(UO_2)_4(OH)_7]^+$ had become the main species with a small amount of $[(UO_2)_3(OH)_7]^-$, $[UO_2(OH)_3]^-$ and $UO_2(OH)_2$. The adsorption was gradually inhibited by electrostatic repulsion between the inactivated *S. cerevisiae* cells and the negatively charged uranium complex anion. Thus pH 2.75 was chosen for the

further studies, where the U(VI) species in solution are dominated by highly mobile UO_2^{2+}.

Effect of Initial U(VI) Concentration and Adsorption Isotherm

The biosorption experiment was investigated over the initial U(VI) concentration range of 5-200 mg/L and the equilibrium data were evaluated using adsorption isotherm models. The effect of the initial uranium ion concentration on U(VI) immobilization is shown in Fig. 2. When the initial U(VI) concentration was between 5 to 200 mg/L, the uranium removal efficiency exceeded 92%. U(VI) biosorption capacity increased from 0.9 to 31.8 mg/g with increasing U(VI) concentration over 5 to 200 mg/L, indicating that the adsorbent had not reached saturation in the experiment. Previous studies reported that the collision frequency between metal ions and the adsorbent increased with increasing initial metal ion concentration, resulting in an enhanced adsorption process [39]. The maximum U(VI) removal efficiency and biosorption capacity in our experiment were 96.8% and 31.8 mg/g, respectively.

Adsorption isotherm provides important information on how the adsorbate molecules are distributed between the liquid and solid phases while the adsorption process reaches equilibrium [40]. The biosorption data were fitted to four different isotherm models viz. Langmuir, Freundlich, Temkin and Dubinin-Radushkevich (D-R) isotherms, as shown in Fig. 3. The isotherm parameters calculated from the four models are presented in Table 1. Correlation coefficient (R^2) values were used to determine the best fit model among the four models tested.

The Langmuir model hypothesized monolayer type adsorption and assumed that all active sites on the adsorbent surface have the same level of attraction to the adsorbate. The Langmuir model is expressed by the equation:

$$\frac{C_e}{q_e} = \frac{1}{K_L \cdot q_{max}} + \frac{C_e}{q_{max}} \qquad (5)$$

...where C_e (mg/L) is the equilibrium concentration of U(VI) ions in solution, q_e (mg/g) is the equilibrium adsorption capacity, q_{max} (mg/g) is the theoretical maximum adsorption capacity and K_L (L/mg) is the Langmuir constant.

The Freundlich isotherm is an empirical equation based on adsorption on a heterogeneous surface with a non-uniform distribution of adsorption energy [41]. It can be written as follows:

$$ln q_e = ln K_F + \frac{1}{n} ln C_e \qquad (6)$$

...where K_F is Freundlich constant, 1/n is the heterogeneity factor representing the intensity of biosorption.
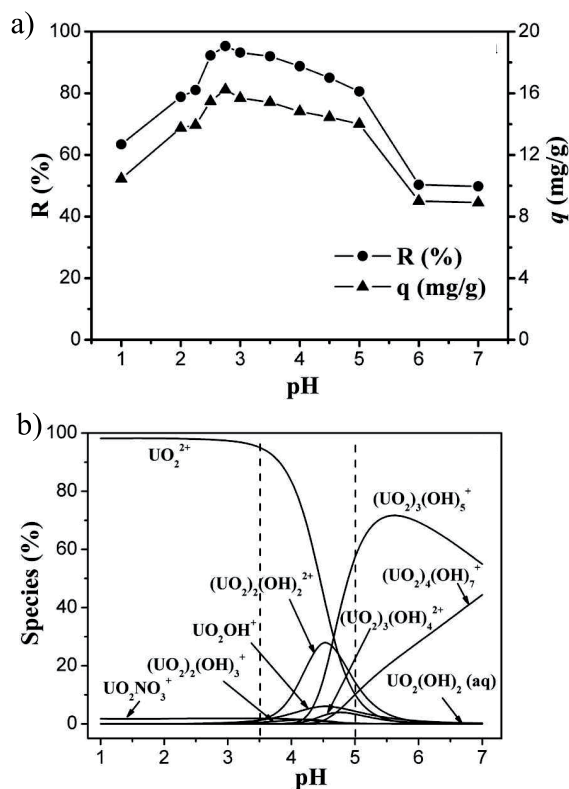

Fig. 1. a) Effect of initial pH on biosorption of U(VI) by inactivated *S. cerevisiae* (U(VI) concentration: 100 mg/L; temperature: 25ºC; inactivated *S. cerevisiae* dosage: 5 g/L; contact time: 60 min), and b) relative species distribution of 100 mg/L U(VI) calculated by Visual MINTEQ 3.1

The Temkin isotherm assumes that the heat of adsorption of all molecules in the layer decrease linearly [42-43]. This model can be written in the following linear form:

$$q_e = \frac{RT}{b} lnK_T + \frac{RT}{b} lnC_e \qquad (7)$$

...where R (8.314 J/mol·K) is the general gas constant, T (K) is absolute temperature, K_T (L/g) is the Temkin isotherm equilibrium binding constant and b is the Temkin isotherm constant.

The Dubinin-Radushkevich (D-R) isotherm is based on the Polanyl potential theory, which expresses the adsorption mechanism with a Gaussian energy distribution onto a heterogeneous surface [44]. The D-R isotherm is expressed as:

$$lnq_e = lnq_{max} - \beta \cdot \varepsilon^2 \qquad (8)$$

...where β is D-R isotherm constant related to mean sorption energy. The parameter ε can be found from Eq. (9):

$$\varepsilon = RT \cdot ln\left(1 + \frac{1}{C_e}\right) \qquad (9)$$

The adsorption energy (E) can be evaluated as follows,

$$E = \frac{1}{(2\beta)^{0.5}} \qquad (10)$$

The magnitude of E is in the range of 1-8 and 9-16 kJ/mol for the physical and ion exchange, respectively [45].

The correlation coefficient (R^2) values of the Langmuir, Temkin and D-R isotherms all deviated from 1.0, which indicated that biosorption of U(IV) by inactivated *S. cerevisiae* did not coincide with
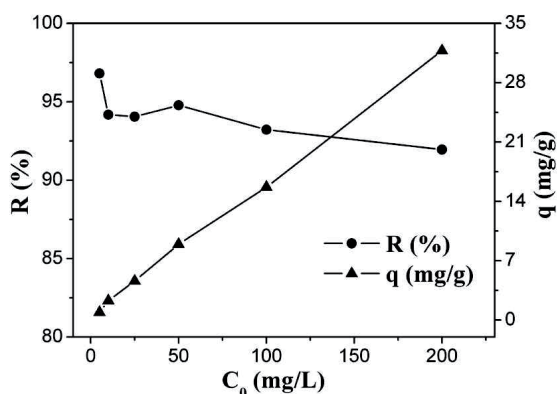
these three isotherms. By contrast, the R^2 value of the Freundlich isotherm model was closer to 1.0, showing that the Freundlich isotherm was more

Fig. 2. Effect of initial U(VI) concentration on the biosorption of U(VI) by inactivated *S. cerevisiae* (initial solution pH: 2.75; temperature: 25ºC; inactivated *S. cerevisiae* dosage: 5 g/L; contact time: 60 min)
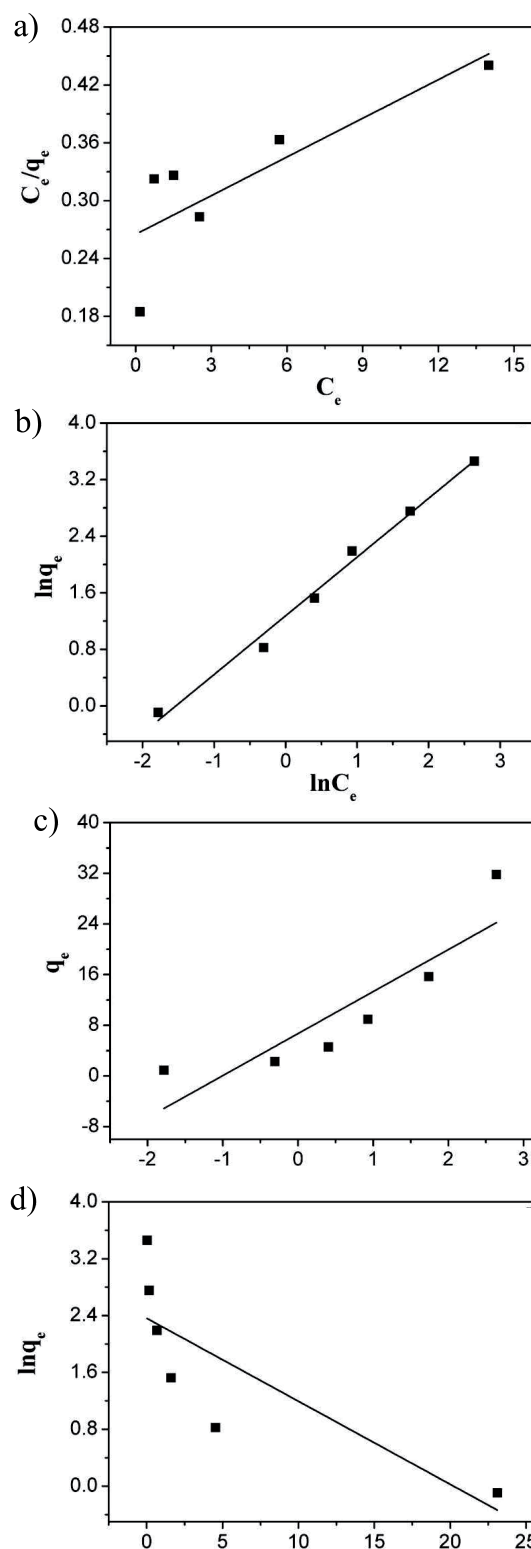
Fig. 3. a) Langmuir adsorption isotherm, b) Freundlich adsorption isotherm, c) Temkin adsorption isotherm, d) D-R adsorption isotherm (initial solution pH: 2.75; temperature: 25ºC; inactivated *S. cerevisiae* dosage: 5 g/L; contact time: 60 min; U(VI) concentration = 5-200 mg/L; solution volume = 20 mL).

Table 1. Isotherm parameters for the biosorption of U(VI) on inactivated *S. cerevisiae*.

Adsorption isotherm	Parameter	Value
Langmuir	q_{max}(mg/g)	74.8503
	K_L (L/mg)	0.0504
	R^2	0.5958
Frendulich	K_F (mg/g)	3.5793
	1/n	0.8303
	R^2	0.9881
Temkin	K_T (L/mg)	2.7464
	RT/b	6.6317
	R^2	0.7330
Dubinin-Radushkevich (D-R)	q_{max}(mg/g)	10.6152
	E (kJ/mol)	2.0691
	R^2	0.5718

Fig. 4. Effect of temperature on the biosorption of U(VI) by inactivated *S. cerevisiae* and the plot of ln K_d *versus* 1/T (U(VI) concentration: 100 mg/L; biomass dosage: 5 g/L; contact time: 60 min; initial solution pH: 2.75).

suitable for describing the adsorption process. The result also indicated that the biosorption of uranium by the inactivated *S. cerevisiae* biomass occurred on a heterogeneous surface where different sites could have different energies. Furthermore, K_F = 3.5793 and 1/n = 0.8303 (less than 1) showed that the separation of U(VI) ions was easy from aqueous solution, suggesting that the immobilization of U(VI) on inactivated *S. cerevisiae* was favorable under experimental conditions [25].

Because neither the Langmuir model nor the D-R model were a good fit for the biosorption process, the q_{max} calculated from the Langmuir and D-R models are quite different from the experimental results, demonstrating that uranium biosorption on the inactivated *S. cerevisiae* did not occur as a single physical or chemical adsorption.

Effect of Temperature on Biosorption of U(VI)

The effect of temperature on the biosorption of U(VI) by inactivated *S. cerevisiae* was studied over the temperature range of 288-313 K. As shown in Fig. 4, U(VI) removal efficiency and biosorption capacity were
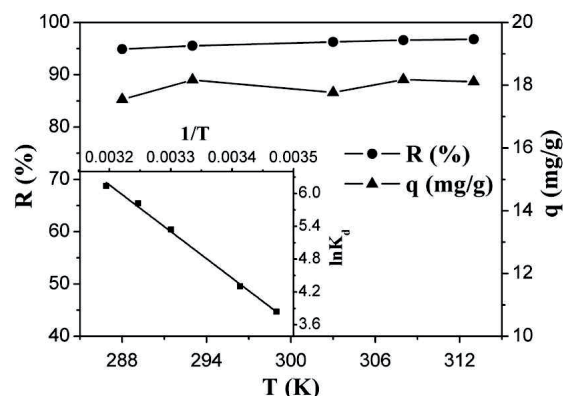
almost constant with increasing temperature, which suggested that uranium biosorption by inactivated *S. cerevisiae* was independent of temperature.

Thermodynamic parameters of the adsorption process, such as enthalpy (ΔH^0), entropy (ΔS^0) and Gibbs free energy (ΔG^0) are important indicators for the practical application of U(VI) biosorption by microbes. The thermodynamic parameters can be calculated by the following equations [46]:

$$lnK_d = \frac{\Delta S^0}{R} - \frac{\Delta H^0}{RT} \qquad (11)$$

$$\Delta G^0 = \Delta H^0 - T \cdot \Delta S^0 \qquad (12)$$

...where K_d (=q_e/C_e) is the distribution coefficient, ΔH^0 (kJ/mol), ΔS^0 (J/mol·K) and ΔG^0 (kJ/mol) are the enthalpy, entropy, and Gibbs free energy, respectively.

The linear variation of lnK_d *versus* 1/T is shown in Fig. 4. Values of ΔH^0, ΔS^0 and ΔG^0 for the adsorption of uranium (VI) by inactivated *S. cerevisiae* are given in Table 2. The negative values for ΔG^0 proved the feasibility as well as the spontaneity of the U(VI) adsorption by inactivated *S. cerevisiae*. Generally, the value of ΔG^0 is in the range of 0 ~ -20 kJ/mol and -80 ~ -400 kJ/mol for physical and chemical sorption, respectively [39]. Values of ΔG^0 in the experiment were between 0 ~ -20 kJ/mol, indicating that U(VI)

Table 2. Thermodynamic parameters for the biosorption of U(VI) by inactivated *S. cerevisiae*.

Temperature (K)	G^0(kJ/mol)	S^0(J/mol·K)	H^0(kJ/mol)	R^2
288	-9.2	278.0	70.9	
293	-10.6	278.0	70.9	
303	-13.4	278.0	70.9	0.9963
308	-14.7	278.0	70.9	
313	-16.1	278.0	70.9	

biosorption by inactivated *S. cerevisiae* may be controlled by physical sorption. The positive value of ΔS^0 showed that the affinity between U(VI) and inactivated *S. cerevisiae* increased and the system randomness also increased. Furthermore, positive entropy is beneficial to the complexation and stability of sorption. The value of ΔH^0 at 70.9 kJ/mol suggested that U(VI) adsorption by inactivated *S. cerevisiae* was an endothermic process and the adsorption process might be controlled by chemical sorption [47].

Effect of Contact time and Biosorption Kinetics

The biosorption kinetics of U(VI) on inactivated *S. cerevisiae* were measured and results are shown in Fig. 5. As can be seen from Fig. 5a, two stages of U(VI) removal process were observed in the experiment: the first stage occurred from 0 - 5 min and was a fast adsorption stage with U(VI) removal efficiency from 0 to 85.3%, while the second stage occurred during 5-60 min with slower adsorption and U(VI) removal efficiency from 85.3% to 89.4%. After 60 min, the removal of U(VI) by inactivated *S. cerevisiae* was almost constant, which showed that the adsorption process reached an equilibrium state.

To further understand the biosorption mechanism of U(VI) by inactivated *S. cerevisiae*, a pseudo first-order model, pseudo second-order model and an intra-particle diffusion model were used to describe the rate-controlling mechanism of the adsorption process. The liner forms of the pseudo first-order kinetic model, pseudo second-order kinetic model and intra-particle diffusion model are given in equation (13), (14) and (15), respectively.

$$\ln\left(q_e - q_t\right) = \ln q_e - k_1 t \tag{13}$$

$$\frac{t}{q_t} = \frac{1}{k_2 q_e^2} + \frac{t}{q_e} \tag{14}$$

$$q_t = k_w t^{0.5} \tag{15}$$

...where q_t (mg/L) is the biosorption capacity at time t, k_1 (min^{-1}) is the pseudo first-order kinetic rate constant, k_2 (g/mg·min) is the pseudo second-order kinetic rate constant, and k_W (mg/g·min$^{1/2}$) is the intra-particle diffusion rate constant.

The fitted curves and parameters from the U(VI) adsorption by inactivated *S. cerevisiae* using the above-mentioned three kinetic models are shown in Fig. 5(b-d) and Table 3. Comparing the calculated correlation coefficient (R^2) from the three kinetic models, it can be seen that the pseudo second-order model gave a very good correlation coefficient (R^2 = 0.9999), while the pseudo first-order model poorly matched the biosorption experimental data, suggesting

that the pseudo second-order model best describes U(VI) adsorption by inactivated *S. cerevisiae*. The pseudo second-order kinetic model also indicated that the rate-limiting step in the biosorption of U(VI) by
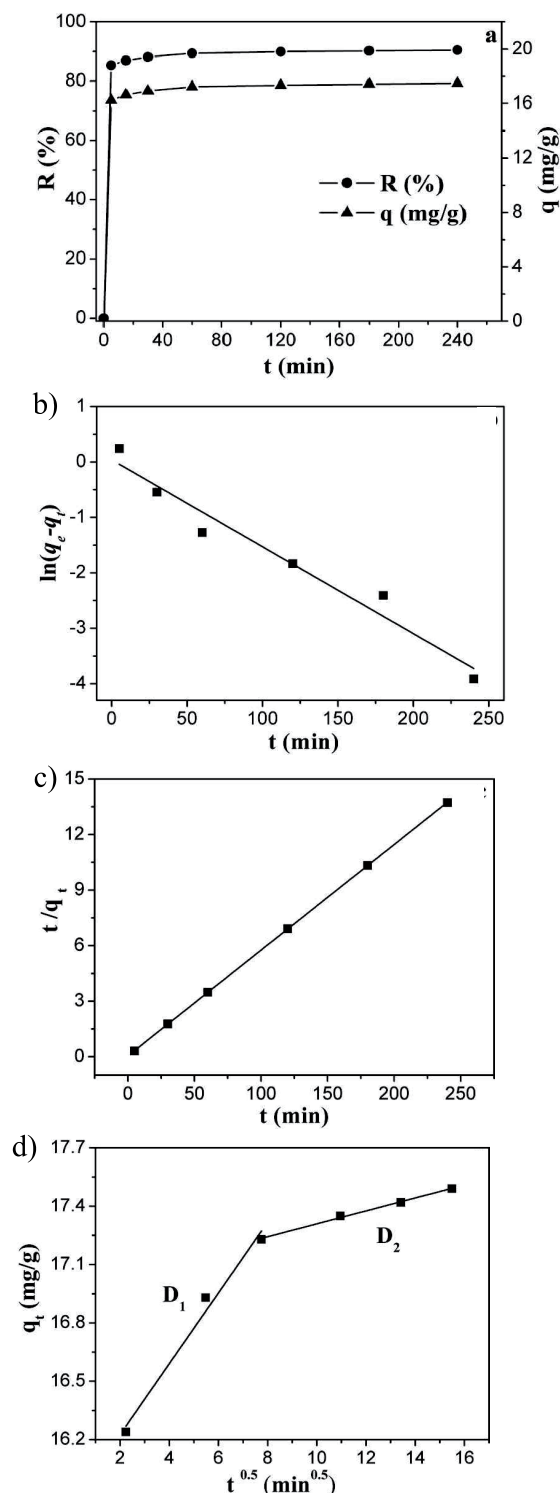

Fig. 5. Kinetic models of U(VI) biosorption by inactivated *S. cerevisiae* a) Effect of contact time on U(VI) adsorption by inactivated *S. cerevisiae*; b) pseudo first-order model; c) pseudo second-order model; d) intraparticle diffusion model; U(VI) concentration: 100 mg/L; biomass dosage: 5 g/L; initial solution pH: 2.75; temperature: 25ºC.

Table 3. Parameters of the kinetic models for U(VI) adsorption.

Models	Parameters	
Pseudo-first-order model	$k_1(\text{min}^{-1})$	0.0157
	$q_e(\text{mg/g})$	1.0375
	R^2	0.9525
Pseudo-second-order model	$k_2(\text{g/mg·min})$	0.0642
	$q_e(\text{mg/g})$	17.5285
	R^2	0.9999
Intraparticle diffusion	K_W	3.0136
	R^2	0.7847

Fig. 6. The residual U(VI) concentration and U(VI) total removal efficiencyusing gradient descent biosorption by inactivated *S. cerevisiae* – U(VI) concentration: 100 mg/L; biomass dosage: 5 g/L; initial solution pH: 2.75; temperature: 25ºC; contact time: 60 min.

inactivated *S. cerevisiae* may be chemical sorption involving valency forces through sharing or exchange of electrons between the sorbent and sorbate [48]. The adsorption capacity $q_{e,cal}$ (17.5 mg/g) calculated from the pseudo second-order kinetic model was close to the experimental value $q_{e,exp}$ (17.2 mg/g), indicating that equilibrium of U(VI) biosorption by inactivated *S. cerevisiae* was established in 60 min.

Fig. 5d shows that the relationship between q_t and $t^{0.5}$ of the intra-particle diffusion model was not linear, suggested that the biosorption of U(VI) by inactivated *S. cerevisiae* was controlled by several adsorption mechanisms. It is worth noting that the intra-particle diffusion plot could be divided into two straight segments, which suggests two mechanisms are involved in the U(VI) biosorption process. The first segment (D_1) was controlled by membrane diffusion, where U(VI) ions were rapidly adsorbed on the outer surface of the cells. Once the first segment reached saturation, U(VI) ions may have begun to combine with functional groups such as carboxyl, amide or amino groups on the cell surface, where intra-particle diffusion was the rate-limiting step (D_2).

Thus, both membrane diffusion and intra-particle diffusion contributed to the rate-limiting step during the adsorption process of U(VI) by inactivated *S. cerevisiae*.
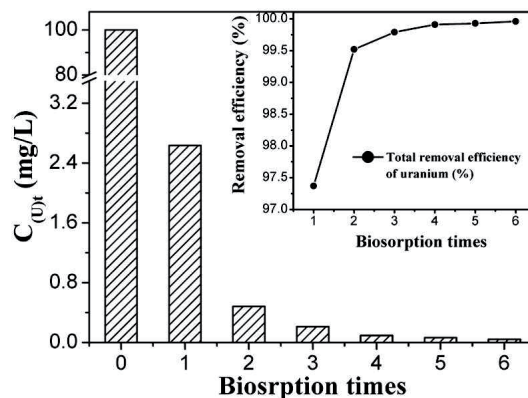
Gradient Descent Biosorption

The residual U(VI) concentration and U(VI) total removal efficiency in the gradient descent biosorption by inactivated *S. cerevisiae* are shown in Fig. 6. The results showed that uranium removal efficiency reached approximately 99.97% after 6 rounds of biosorption. The 100 mg/L uranium in solution was reduced to less than 0.05 mg/L, indicating that the residual concentration of U(VI) in the supernatant met the Chinese Environment Protection Ministry maximum contaminant limit for drinking water. Thus, gradient descent biosorption is a feasible method for the removal of uranium to the discharge level.

Reduction and Enrichment for Uranium

Volume reduction of uranium solutions and weight reduction of the adsorbent were investigated and the results are shown in Table 4. As seen from the experiment, approximately 95% of the uranium was adsorbed on inactivated *S. cerevisiae* after biosorption ($C_{U(VI)}$=100 mg/L) and the residual 5% of the uranium

Table 4. VRR and WRR after ashing process.

Content	A-1	A-2	A-3
U(VI) solution volume (mL) before biosorption	250.0	250.0	250.0
Ash volume (mL)	0.0558	0.0573	0.0539
Volume reduction ratio	4480	4363	4638
V_{RR} (average)	4494		
Sediment weight after biosorption (g)	1.1255	1.1523	1.1750
Ash weight (g)	0.0558	0.0573	0.0539
Weight reduction ratio	20.2	20.1	21.8
W_{RR} (average)	20.7		

in solution was ignored. Therefore, the calculated ratio of uranium solution volume reduction was approximately 4500 times and the ratio of biosorbent weight reduction was approximately 20 times. The results revealed that treatment of the adsorbent by ashing could lead to a great reduction in the volume ratio for radioactive effluent, making the process very useful for geological disposal.

In the following, the enrichment of uranium in the ash was examined. Fig. 7(a-b) show SEM micrographs
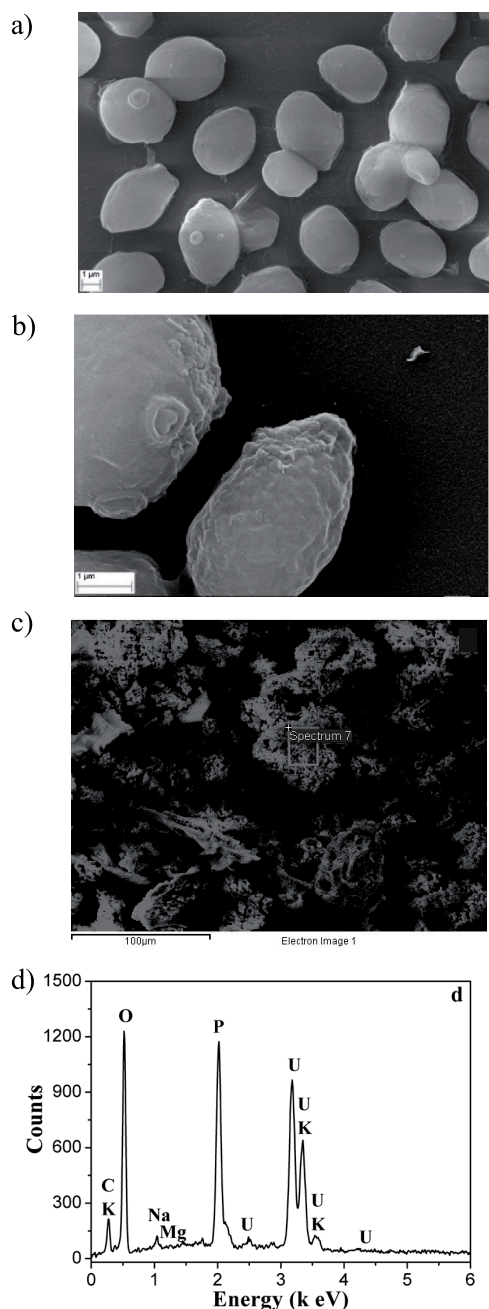
a)

b)

c)

d)

Fig. 7. SEM images of a) inactivated *S. cerevisiae* before and b) after biosorption of uranium and c) U(VI)-loaded inactivated *S. cerevisiae* cells after ashing; d) EDS analysis of the ash – U(VI) concentration: 100 mg/L; biomass dosage: 5 g/L; initial solution pH: 2.75; temperature: 25ºC; contact time: 60 min; U(VI) solution volume: 250 mL.

of inactivated *S. cerevisiae* cells before and after exposure to 100 mg/L of U(VI) for 60 min, respectively. The inactivated *S. cerevisiae* control cells had an intact shape and smooth surface. After U(VI) treatment, the surface of the inactivated *S. cerevisiae* cells was covered with numerous irregular clusters of nanoparticles. Fig. 7(c-d) shows SEM micrographs and EDS spectra of U(VI)-loaded inactivated *S. cerevisiae* cells after ashing. Some strong uranium peaks emerged around energy level of 2.5 ~ 3.5 keV in the EDS spectra. The uranium content in the ash (q_{ash}) reached 50.8% and the enrichment factor of the uranium was about 30 compared to the inactivated *S. cerevisiae* cell sediments ($q_{t=60} \approx 17$ mg/g). This means that the ashing process could lead to uranium enrichment as well as a large volume and weight reduction ratio. Therefore, the ashing process appears to be beneficial for metal recovery in addition to the reduction process.

During ash precipitation, the elements of U, C, O, P, Na, K, Mg were the main elements, the other elements are few.

Speciation of Uranium in Ash

In order to investigate the speciation of uranium in ash, the ash was analyzed by XRD. The results demonstrated that the X-ray powder diffraction peak curve of the ash sample without loaded uranium (control) was a bread peak, which revealed the amorphous characteristics of the ash and the high content organic components (Fig. 8). However, some obvious diffraction peaks were detected in the ash when uranium was adsorbed onto inactivated *S. cerevisiae*. The XRD analysis showed that uranium existed in ash in the form of uranium phosphate and $KPUO_6 \cdot 3H_2O$. The results also mean that uranium in solution can exist as stable uranium crystals after biosorption and ashing treatment, which is convenient for separation and advanced treatment, and provides important information for the disposal of actual uranium-containing wastewater.
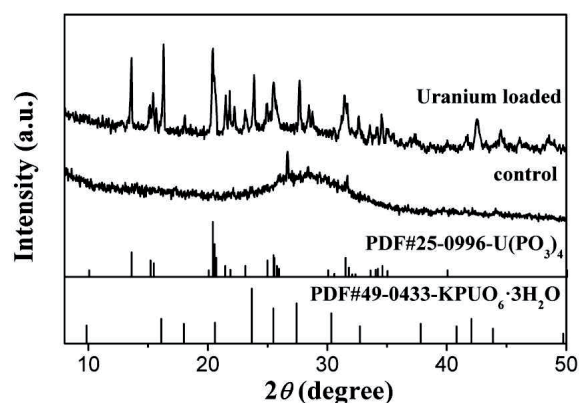

Fig. 8. XRD spectra of ash samples before and after biosorption of uranium.

Conclusions

In the present study, the use of inactivated *S. cerevisiae* in the removal of uranium(VI) was investigated. The U(VI) biosorption process on inactivated *S. cerevisiae* has been suggested to be influenced by experimental conditions such as solution pH, initial concentration of U(VI), temperature and contact time. The results revealed that inactivated *S. cerevisiae* biomass was able to adsorb uranium. The maximum removal efficiency and biosorption capacity for uranium were 96.8% and 31.8 mg/g, respectively. Solution pH is an important parameter that affects the biosorption process and the optimum biosorption pH value in the study was found to be 2.75. The biosorption process was well described by the Freundlich isotherm model. Thermodynamic investigation revealed that the biosorption of U(VI) on inactivated *S. cerevisiae* was a spontaneously endothermic process that was independent of temperature. Kinetics studies indicated that uranium biosorption occurred in 60 min and followed a pseudo-second-order kinetics model. Both membrane diffusion and intra-particle diffusion contributed to the rate-limiting step during the adsorption of U(VI) on inactivated *S. cerevisiae*. In the gradient descent process, 100 mg/L of uranium was reduced to less than 0.05 mg/L with constant replacement and 6 rounds of gradient descent. The ashing process resulted in a volume reduction ratio 4500 times of the uranium solution and a 20 times weight reduction ratio of the biosorbent as well as an enrichment ratio of approximately 30 times for uranium in ash. XRD results showed that the species of uranium that existed in the ash was uranium phosphate and $KPUO_6 \cdot 3H_2O$. The results revealed that biosorption combined with the ashing process could be beneficial for nuclide and heavy metal disposal.

Conflict of Interest

The authors declare no conflict of interest.

Acknowledgements

References

1. BAYRAMOGLU G., ARICA M.Y. Amidoxime functionalized *Trametes trogii* pellets for removal of uranium(VI) from aqueous medium. J. Radioanal. Nucl. Chem. **307** (1), 373, **2016**.
2. SHAO L., WANG X.F., REN Y.M., WANG S.F., ZHONG J.R., CHU M.F., TANG H., LUO L.Z., XIE D.H. Facile fabrication of magnetic cucurbit[6]uril/graphene oxide composite and application for uranium removal. Chem. Eng. J. **286**, 311, **2016**.
3. PANG C., LIU Y.H., CAO X.H., LI M., HUANG G.L., HUA R., WANG C.X., LIU Y.T., AN X.F. Biosorption of uranium(VI) from aqueous solution by dead fungal biomass of *Penicillium citrinum*. Chem. Eng. J. **170** (1), 1, **2011**.
4. HUANG W.B., NIE X.Q., DONG F.Q., DING C.C., HUANG R., QIN Y.L., LIU M.X., SUN S.Y. Kinetics and pH-dependent uranium bioprecipitation by *Shewanella putrefaciens* under aerobic conditions. J. Radioanal. Nucl. Chem. **312** (3), 531, **2017**.
5. GORMAN-LEWIS D., ELIAS P.E., FEIN J.B. Adsorption of aqueous uranyl complexes onto *Bacillus subtilis* cells. Environ. Sci. Technol. **39** (13), 4906, **2005**.
6. YANG G., DONG F.Q., LIU M.X., NIE X.Q., ZONG M.R., PENG C.H., CHEN H., WEI H.F., WANG P.P., ZHANG W. Interactive effect of radioactive and heavy-metal contamination on soil enzyme activity in a former Uranium mine. Pol. J. Environ. Stud. **27** (3), 1343, **2018**.
7. USEPA. EPA Integrated Risk Information System (IRIS), Electronic Database. USEPA, Washington DC, **1996**.
8. AHMED S.H., SHEIKH E.M., MOTSY A.M.A. Potentiality of uranium biosorption from nitric acid solutions using shrimp shells. J. Environ. Radioact. **134**, 120, **2014**.
9. BAYRAMOGLU G., BEKTAS S., ARICA M.Y. Biosorption of heavy metal ions on immobilized white-tot fungus *Trametes versicolor*. J. Hazard. Mater. **101** (3), 285, **2003**.
10. DMITRIEV S.A., KARLIN Y.V., MARYAKHIN M.A., MYASNIKOV Y.G., SLASTENNIKOV Y.T. Liquid radwaste concentration by evaporation from porous plates. At. Energy, **106** (4), 266, **2009**.
11. JULIANO P., SWIERGON P., LEE K.H., GEE P.T., CLARKE P.T., AUGUSTIN M.A. Effects of pilot plant-scale ultrasound on palm oil separation and oil quality. J. Am. Oil. Chem. Soc. **90** (8), 1253, **2013**.
12. SINGHAL R.K., BASU H., PIMPLE M.V., MANISHA V., BASAN M.K.T., REDDY A.V.R. Spectroscopic determination of U(VI) species sorbed by the *Chlorella (Chlorella pyrenoidosa)* fresh water algae. J. Radioanal. Nucl. Chem. **298** (1), 587, **2013**.
13. HE J.S., CHEN J.P. A comprehensive review on biosorption of heavy metals by algal biomass: materials, performances, chemistry, and modeling simulation tools. Bioresour. Technol. **160**, 67, **2014**.
14. AMBASHTA R.D., SILLANPAA M.E.T. Membrane purification in radioactive waste management: a short review. J. Environ. Radioact. **105**, 76, **2012**.
15. SAINI A.S., MELO J.S. Biosorption of uranium by melanin: Kinetic, equilibrium and thermodynamic studies. Bioresour. Technol. **149**, 155, **2013**.

16. KULKARNI S., BALLAL A., APTE S.K. Bioprecipitation of uranium from alkaline waste solutions using recombinant *Deinococcus radiodurans*. J. Hazard. Mater. **262**, 853, **2013**.

17. BAI J., YIN X.J., ZHU Y.F., FAN F.L., WU X.L., TIAN W., TAN C.M., ZHANG X., WANG Y., CAO S.W., FAN F.Y., QIN Z., GUO J.S. Selective uranium sorption from salt lake brines by amidoximated *Saccharomyces cerevisiae*. Chem. Eng. J. **283**, 889, **2016**.

18. GOK C., AYTAS S., SEZER H. Modeling uranium biosorption by *Cystoseira* sp. and application studies. Sep. Sci. Technol. **52** (5), 792, **2016**.

19. ÖZDEMIR S., ODUNCU M.K., KILINC E., SOYLAK M. Tolerance and bioaccumulation of U(VI) by *Bacillus mojavensis* and its solid phase preconcentration by *Bacillus mojavensis* immobilized multiwalled carbon nanotube. J. Environ. Manage. **187**, 490, **2017**.

20. ZINICOVSCAIA I., SAFONOV A., TREGUBOVA V., ILIN V., FRONTASYEVA M.V., DEMINA L. Bioaccumulation and biosorption of some selected metals by bacteria *Pseudomonas putida* from single- and multi-component systems. Desalin. Water. Treat. **74**, 149, **2017**.

21. KHANI M.H., KESHTKAR A.R., GHANNADI M., PAHLAVANZADEH H. Equilibrium, kinetic and thermodynamic study of the biosorption of uranium onto *Cystoseria indica* algae. J. Hazard. Mater. **150** (3), 612, **2008**.

22. KIM I., LEE M., WANG S. Heavy metal removal in groundwater originating from acid mine drainage using dead *Bacillus drentensis* sp. immobilized in polysulfone polymer. J. Environ. Manage. **146**, 568, **2014**.

23. BAGDA E., TUZEN M., SARI A. Equilibrium, thermodynamic and kinetic investigations for biosorption of uranium with green algae (*Cladophora hutchinsiae*). J. Environ. Radioact. **175-176**, 7, **2017**.

24. LIU M.X., DONG F.Q., YAN X.Y., ZENG W.M., HOU L.Y., PANG X.F. Biosorption of uranium by *Saccharomyces cerevisiae* and surface interactions under culture conditions. Bioresour. Technol. **101** (22), 8573, **2010**.

25. BAYRAMOGLU G., ÇELIK G., ARICA M.Y. Studies on accumulation of uranium by fungus *Lentinus sajor-caju*. J. Hazard. Mater. **136** (2), 345, **2006**.

26. CARVAJAL D.A., KATSENOVICH Y.P., LAGOS L.E. The effects of aqueous bicarbonate and calcium ions on uranium biosorption by *Arthrobacter* G975 strain. Chem. Geol. **330-331**, 51, **2012**.

27. LI X.L., DING C.C., LIAO J.L., LAN T., LI F.Z., ZHANG D., YANG J.J., YANG Y.Y., LUO S.Z., TANG J., LIU N. Biosorption of uranium on *Bacillus* sp. dwc-2: preliminary investigation on mechanism. J. Environ. Radioact. **135**, 6, **2014**.

28. WANG T.S., ZHENG X.Y., WANG X.Y., LU X., SHEN Y.H. Different biosorption mechanisms of uranium(VI) by live and heat-killed *Saccharomyces cerevisiae* under environmentally relevant conditions. J. Environ. Radioact. **167**, 92, **2017**.

29. WANG J.L., CHEN C. Biosorption of heavy metals by *Saccharomyces cerevisiae*: A review. Biotechnol. Adv. **24** (5), 427, **2006**.

30. RAJ K., PRASAD K.K., BANSAL N.K. Radioactive waste management practices in India. Nucl. Eng. Des. **236** (7-8), 914, **2006**.

31. KIM I.G., KIM S.S., KIM G.N., HAN G.S., CHOI J.W. Reduction of Radioactive Waste from Remediation of Uranium-Contaminated Soil. Nucl. Eng. Technol. **48** (3), 840, **2016**.

32. MIN B.Y., LEE Y.J., YUN G.S., LEE K.W., MOON J.K. Volume reduction of radioactive combustible waste with Oxygen Enriched Incinerator. Ann. Nucl. Energy. **80**, 47, **2015**.

33. ARNAL J.M., SANCHO M., GARCIA-FAYOS B., VERDU G., SERRANO C., RUIZ-MARTINEZ J.T. Declassification of radioactive water from a pool type reactor after nuclearfacility dismantling. Radiat. Phys. Chem. **138**, 72, **2017**.

34. BYKHOVSKII D.N., KOLTSOVA T.I., ROSHCHINSKAYA E.M. Reduction of radioactive waste volume using selective crystallization processes. Radiochemistry, **52** (5), 530, **2010**.

35. CHON J.K., BEAUDOIN V., PITCHER C.S. Conceptual design of volume reduction system for ITER low level radioactive waste. Fusion Eng. Des. **109-111**, 1001, **2016**.

36. NAKASHIO N., HIGUCHI H., MOMMA T., KOZAWA K., TOUHEI T., SUDOU T., MITSUDA M., KUROSAWA S., HEMMI K, ISHIKAWA J., KATO M., SATO M. Trial Operation of the Advanced Volume Reduction Facilities for LLW at JAEA. J. Nucl. Sci. technol. **44** (3), 441, **2007**.

37. KUNCHAM K., NAIR S., DURANI S., BOSE R. Efficient removal of uranium(VI) from aqueous medium using ceria nanocrystals: an adsorption behavioural study. J. Radioanal. Nucl. Chem. **313** (1), 101, **2017**.

38. IKEDA A., HENNIG C., TSUSHIMA S., TAKAO K., IKEDA Y., SCHEINOST A.C., BERNHARD G. Comparative study of Uranyl (VI) and – (V) carbonato complexes in an aqueous solution. Inorg. Chem. **46** (10), 4212, **2007**.

39. BAYRAMOGLU G., AKBULUT A., ARICA M.Y. Study of polyethyleneimine- and amidoxime-functionalized hybrid biomass of *Spirulina* (*Arthrospira*) *platensis* for adsorption of uranium (VI) ion. Environ. Sci. Pollut. Res. **22** (22), 17998, **2015**.

40. YI Z.J., YAO J., ZHU M.J., CHEN H.L., WANG F., LIU X. Biosorption characteristics of *Ceratophyllum demersum* biomass for removal of uranium(VI) from an aqueous solution [J]. J. Radioanal. Nucl. Chem. **313** (1), 19, **2017**.

41. BAKATULA E.N., CUKROWSKA E.M., WEIERSBYE I.M., MIHALY-COZMUTA L., PETER A., TUTU H. Biosorption of trace elements from aqueous systems in gold mining sites by the filamentous green algae (*Oedogonium sp.*). J. Geochem. Explor. **144**, 492, **2014**.

42. TEMKIN M.I. Kinetics of ammonia synthesis on promoted iron catalyst. Acta. Physiochim. URSS. **12**, 327, **1940**.

43. AHARONI C., UNGARISH M. Kinetics of activated chemisorption. Part 2.-theoretical models. J. Chem. Soc. Faraday.Trans. **73**, 456, **1977**.

44. GUNAY A., ARSLANKAYA E., TOSUN I. Lead removal from aqueous solution by natural and pretreated clinoptilolite: adsorption equilibrium and kinetics. J. Hazard. Mater. **146** (1-2), 362, **2007**.

45. EL-KAMASH A.M., ZAKI, A.A., ABED EI GELEEL M. Modeling batch kinetics and thermodynamic of zinc and cadmium ions removal from waste solutions using synthetic zeolite A. J. Hazard. Mater. **127** (1-3), 211, **2005**.

46. GOK C., AYTAS S. Biosorption of uranium(VI) from aqueous solution using calcium alginate beads. J. Hazard. Mater. **168** (1), 369, **2009**.

47. KILILC M., YAZILCIL H., SOLAK M. A Comprehensive study on removal and recovery of copper(II) from aqueous solutions by NaOH-pretreated *Marrubium globosum*

ssp. *globosum* leaves power: potential for utilizing the copper(II) condensed desorption solutions in agricultural applications. Bioresour. Technol. **100** (7), 2130, **2008**.

48. MOTSI T., ROWSON N.A., SIMMONS M.J.H. Adsorption of heavy metals from acid mine drainage by natural zeolite. Int. J. Miner. Process. **92** (1-2), 42, **2009**.